Decays of mass-separated ^{139}Xe and ^{139}Cs

M. A. Lee* and W. L. Talbert, Jr.†

Ames Laboratory—United States Department of Energy and Department of Physics, Iowa State University, Ames, Iowa 50010

(Received 15 June 1979)

The β and subsequent γ decays of ^{139}Xe and ^{139}Cs have been studied using an on-line isotope separator system. Ge(Li) γ-ray singles and Ge(Li)-Ge(Li) γ-γ coincidence measurements were used to construct level schemes for ^{139}Cs and ^{139}Ba. For the decay of ^{139}Xe, 213 of 230 observed γ-ray transitions have been placed in a level scheme for ^{139}Cs with 55 excited states. For the decay of ^{139}Cs, 167 of 179 observed γ-ray transitions are placed in a level scheme for ^{139}Ba with 59 excited states. The Q values for the β decays of ^{139}Xe and ^{139}Cs were determined from Ge(Li) plastic scintillator coincidence measurements as 5.02 ± 0.06 and 4.29 ± 0.07 MeV, respectively. Ground-state β branches were deduced for the ^{139}Xe and ^{139}Cs decays using relative γ-ray intensities. Spin and parity assignments for levels in ^{139}Cs and ^{139}Ba have been deduced using β-decay logft values, γ-ray transition rates, and reaction data in the literature. Interpretation of some of the energy levels is made from a shell-model viewpoint.

[RADIOACTIVITY ^{139}Xe, ^{139}Cs [from ^{235}U(n,f)]; measured E_γ, I_γ, $\gamma-\gamma$ coin., Q_β, Ge(Li), and plastic scint. detectors. ^{139}Cs, ^{139}Ba deduced levels, J, π, logft. ^{139}Xe, ^{139}Cs deduced ground-state β branches. Mass-separated ^{139}Xe activity.]

I. INTRODUCTION

The decays of ^{139}Xe and ^{139}Cs have been studied at the TRISTAN on-line isotope separator facility as part of a systematic study of the short-lived gaseous fission products and their daughters in the region of $Z = 50$ and $N = 82$. The results of a study of the γ-ray deexcitations following these decays and the level schemes deduced for ^{139}Cs and ^{139}Ba are presented; in a previous paper the results of the Q_β measurements for these decays, among others, were reported.[1]

The use of isotope separator on-line techniques in the study of the ^{139}Xe decay was initially reported by Holm *et al.* who employed Ge(Li) γ-ray detectors and an anthracene β detector.[2] They deduced a level scheme for ^{139}Cs in which 15 γ-ray transitions were placed among seven excited levels. In a later study of this decay, Alväger *et al.* placed eleven γ-ray transitions among five excited levels.[3] At this laboratory, Cook and Talbert deduced a level scheme in which 48 transitions were placed among 15 excited levels.[4] No reaction studies leading to levels in ^{139}Cs have been reported. The internal conversion coefficients for a few of the transitions have been measured by Achterberg *et al.*[5] Recently, Ekström *et al.* have reported that the ground-state spin of ^{139}Cs is $\frac{7}{2}$, from on-line atomic-beam magnetic resonance measurements.[6]

The $N = 83$ nucleus ^{139}Ba has been studied extensively through the ^{138}Ba(d,p)^{139}Ba reaction[7-14] by the ^{138}Ba(n,γ)^{139}Ba reaction[15] and by proton elastic scattering from ^{139}La.[16] Only recently has any extensive study of the γ-ray deexcitation following the β decay of ^{139}Cs been carried out. Early work carried out by Aksenov *et al.*[17] and by Zherebin *et al.*[18] involved use of scintillation detectors and resulted in the detection of 13 γ-ray transitions. Monnand *et al.* have recently completed a study of this decay and their results, while significantly different in several details, are in fair agreement with the results of the present work.[19]

In the present work, level schemes for ^{139}Cs and ^{139}Ba are presented. These level schemes were deduced from the γ-ray energy and intensity measurements and γ-γ coincidence measurements. The ground-state β branching in the decay of ^{139}Cs was deduced from the γ-ray intensities of the 1283-keV transition in the ^{139}Cs decay and the 165-keV transition in the ^{139}Ba decay, assuming the absolute intensity of 0.22 ± 0.01 for the 165-keV transition recently reported by Gleason.[20] The ground-state β branching intensity for the ^{139}Xe decay was calculated from γ-ray intensity ratios measured in the equilibrium spectrum of ^{139}Xe and ^{139}Cs, using the branching intensities deduced previously for the ^{139}Cs decay. Logft values of the β transitions for both decays were calculated using the β branching intensities deduced from γ-ray intensity imbalances. Tentative spin and parity assignments for the levels in ^{139}Cs and ^{139}Ba are based partly upon logft values using the rules presented by Raman and Gove.[21] A preliminary version of the results presented here has been reported in the latest revision of the Nuclear Data Sheets for $A = 139$ and was used

as the basis for the adopted decay schemes of ^{139}Xe and ^{139}Cs.[22]

II. EXPERIMENTAL PROCEDURES

A. Experimental arrangement

The ^{139}Xe activity was obtained as a fission product of ^{235}U and the ^{139}Cs sources were obtained as daughter products of the ^{139}Xe decay. The fissioning uranium sample was in the form of uranyl stearate which was placed in an external neutron beam of the Ames Laboratory research reactor where the flux was approximately 3×10^9 n/cm^2 s. The gaseous fission products were introduced into the ion source through a 1.5-m transfer line. The isotopic separation was obtained from a 160-cm 90° sector magnet, and the ^{139}Xe ion beam was selected by a slit in the separator focal plane and sent through a switch magnet to a moving tape collector. A plastic scintillator was mounted inside the tape collector and Ge(Li) detectors were placed immediately outside the walls of the tape collector on both sides of the sample. A more complete description of the isotope separator system is available in the literature.[23]

Associated with the tape collector was a daughter analysis system which allowed an experimental cycle to be chosen consisting of periods of beam deposit, delay (for decay of parent activity), tape transport (to daughter activity detector port), and data accumulation. The system provided a preselected time interval for each of these steps so that the times could be chosen to optimize the activity of interest. The computer code ISOBAR was used to calculate the optimum times for these steps and to determine the integrated activity ratios for each of the decays.[24]

B. Data accumulation

For γ-ray detection, Ge(Li) detectors of 58-cm^3 active volume were used. For singles spectra, the energies were measured with 8192-channel resolution. For the γ-γ coincidence experiments, two 4096-channel ADC's were used together with a buffer tape system to record coincidences event by event with high resolution, for later analysis. The plastic scintillator used in the β-γ coincidence experiments was made of Pilot B plastic, and the description of the detector assembly has been reported by Wohn *et al.*[25]

The half-lives for the two decays have been measured by Carlson *et al.*[26] to be 39.68 ± 0.14 s for ^{139}Xe and 556 ± 3 s for ^{139}Cs. Effective separation of the two activities can be obtained with the moving tape collector. For the ^{139}Xe experiment the activity, as calculated from ISOBAR,[24] consisted of 98.0% xenon and 2.0% cesium, while for the ^{139}Cs decay the values were 0.2% xenon, 87.7% cesium, and 12.1% barium. More than 99% of the ^{139}Ba activity was contained in the 165.83-keV transition, so the presence of barium activity presented no major contamination problem.

For each γ-ray singles run, four separate spectra were obtained. The first spectrum was obtained with calibration sources alone and was used to determine the nonlinearities of the system. The second was taken with the calibration sources and the unknown, and these data were used to determine the energies of the more prominent photopeaks in the unknown spectrum. These peaks were then used as calibration points in the spectrum taken with the unknown alone. A background spectrum was taken to determine the occurrence of any γ-ray activity around the reactor environment.

C. Data analysis

The centroids and areas of each of the spectrum peaks were determined through use of a computer program SKEWGAUS which utilizes a nonlinear least-squares fit of the data to a skewed-Gaussian fit function.[27] The centroids and areas were converted into γ-ray energies and intensities through use of a computer program DRUDGE which was prepared by Olson.[28]

The analysis of the γ-γ coincidence data was carried out using the buffer tape system and plots of the coincidence spectra. By playing the magnetic tapes containing the two-parameter data through the buffer tape system, a spectrum of all γ-ray transitions in coincidence with any desired digitally selected gating transition was obtained. This spectrum was visually compared with the spectrum gated by a region of the gating spectrum just adjacent to the peak in question. If a peak in the photopeak-gated spectrum showed a clear enhancement over that displayed in the background-gated spectrum, that transition was considered to be definitely in coincidence with the gating transition, and these are indicated on the level scheme by a solid circle. For weaker peaks, or those for which the enhancement over nearby gates is not as clearly indicated, the coincidence was regarded as being probable and is denoted on the level scheme by an open circle. For brevity, the detailed coincidence results (from 30 gated spectra for the decay of ^{139}Xe, and 35 gates in ^{139}Cs decay) are not presented here, but have been tabulated by Lee[29] and Greenwood.[22] The details of the level schemes

TABLE I. Photopeaks observed in the decay of ^{139}Xe.

Energy (keV)	Relative intensity[a]	Placement (keV)	Energy (keV)	Relative intensity[a]	Placement (keV)
55.7 ±0.3	1.9± 0.5	2119 – 2063	888.6 ±0.5	1.2± 0.6	1831 – 942
71.0 ±0.4	4.6± 1.6	289 – 218	891.76±0.18	3.8± 0.6	891 – 0
103.75±0.06	5.6± 0.4	393 – 289	896.3 ±0.3	3.8± 0.5	1186 – 289
119.4 ±0.4	1.2± 0.4	2304 – 2185	924.5 ±0.6	2.0± 1.1	1816 – 891
121.37±0.08	6.9± 0.6	515 – 393	926.0 ±0.6	1.8± 1.1	2620 – 1693
174.97±0.04	356 ±22	393 – 218	937.9 ±0.4	1.3± 0.3	2754 – 1816
218.59±0.03	1000 ±56	218 – 0	942.61±0.22	2.1± 0.4	942 – 0
225.38±0.07	52 ± 5	515 – 289	946.5 ±0.3	1.7± 0.4	1461 – 515
289.78±0.07	164 ±10	289 – 0	957.3 ±0.4	1.3± 0.4	3924 – 2967
296.53±0.07	389 ±22	515 – 218	961.1 ±0.4	1.4± 0.4	1693 – 732
326.8 ±0.4	1.2± 0.4	2119 – 1793	967.3 ±0.5	1.2± 0.4	1186 – 218
338.86±0.07	10.7± 0.6	732 – 393	970.3 ±0.4	1.4± 0.4	3155 – 2185
356.72±0.08	8.8± 0.6	646 – 289	980.59±0.18	2.9± 0.4	2119 – 1138
393.50±0.06	120 ± 6	393 – 0	986.02±0.11	6.0± 0.5	2585 – 1599
427.4 ±0.4	1.1± 0.4	942 – 515	996.19±0.11	5.8± 0.5	1214 – 218
441.3 ±0.7	1.6± 0.4	1461 – 1020	1001.7 ±0.4	1.4± 0.4	1395 – 393
442.7 ±0.4	2.8± 0.4	732 – 289	1006.25±0.14	4.2± 0.3	1652 – 646
446.8 ±0.3	1.2± 0.4	2099 – 1652	1017.7 ±0.3	2.4± 0.6	3745 – 2727
454.46±0.13	3.5± 0.4	1461 – 1006	1021.4 ±0.6	0.8± 0.4	2620 – 1599
466.8 ±0.3	1.3± 0.3	1652 – 1186	1036.3 ±0.3	1.8± 0.4	3155 – 2119
491.47±0.04	25.8± 1.4	1006 – 515	1046.31±0.15	4.8± 0.6	3375 – 2328
498.2 ±0.5	0.9± 0.4	891 – 393	1067.56±0.24	2.5± 0.5	1461 – 393
505.07±0.08	5.8± 0.5	1020 – 515	1099.4 ±0.5	1.1± 0.5	2119 – 1020
513.88±0.11	15.0± 1.5	732 – 218	1105.6 ±0.3	2.1± 0.4	1395 – 289
515.44±0.14	9.2± 1.5	515 – 0	1114.48±0.12	6.0± 0.6	1508 – 393
549.02±0.04	10.3± 0.6	942 – 393	1137.52±0.10	7.1± 0.5	1652 – 515
565.4 ±0.3	1.1± 0.3	1508 – 942	1149.2 ±0.3	2.2± 0.4	2980 – 1831
569.64±0.22	1.6± 0.3	1461 – 891	1171.5 ±0.4	1.4± 0.4	1461 – 289
589.8 ±0.4	1.1± 0.4	2328 – 1738	1176.3 ±0.6	1.6± 0.6	1395 – 218
595.43±0.13	3.5± 0.4	2103 – 1508	1178.73±0.12	9.0± 0.8	1693 – 515
601.84±0.07	9.3± 0.7	891 – 289	1190.6 ±0.6	0.9± 0.4	2585 – 1395
612.82±0.04	98 ± 5	1006 – 393	1199.43±0.23	2.4± 0.4	2852 – 1652
624.3 ±0.7	1.7± 0.9	2727 – 2103	1206.45±0.10	11.2± 0.9	1599 – 393
626.89±0.11	14.0± 1.2	1020 – 393	1214.9 ±0.4	1.3± 0.4	1214 – 0
646.50±0.07	10.5± 0.8	646 – 0	1219.33±0.21	2.8± 0.4	2727 – 1508
652.28±0.13	4.2± 0.5	942 – 289	1228.8 ±0.5	1.1± 0.4	2967 – 1738
672.39±0.18	2.5± 0.4	891 – 218	1242.88±0.08	10.5± 0.8	2185 – 942
675.79±0.16	2.9± 0.4	2328 – 1652	1259.26±0.09	9.3± 0.7	1652 – 393
699.6 ±0.3	1.6± 0.4	1214 – 515	1273.1 ±0.5	1.1± 0.5	3372 – 2099
710.40±0.18	3.2± 0.5	1652 – 942	1289.47±0.19	7.8± 1.1	1508 – 218
716.96±0.22	3.0± 0.5	1006 – 289	1291.4 ±0.4	3.1± 1.0	4227 – 2936
719.8 ±0.6	1.2± 0.5	2373 – 1652	1297.85±0.19	7.2± 1.1	2304 – 1006
723.84±0.06	32.2± 1.8	942 – 218	1299.8 ±0.9	1.5± 1.0	1693 – 393
730.4 ±0.3	4.1± 0.9	1020 – 289	1309.4 ±0.8	1.6± 1.0	1599 – 289
732.42±0.06	31.4± 1.9	732 – 0	1316.4 ±0.4	1.9± 0.5	1831 – 515
745.16±0.07	9.5± 0.6	1138 – 393	1324.38±0.21	3.3± 0.5	3155 – 1831
761.04±0.16	3.6± 0.5	1652 – 891	1344.93±0.07	20.4± 1.2	1738 – 393
773.4 ±0.5	1.7± 0.6	2373 – 1599	1351.6 ±0.4	1.7± 0.5	3775 – 2423
775.6 ±0.4	1.8± 0.6	1508 – 732	1362.91±0.12	5.1± 0.5	1652 – 289
783.1 ±0.5	1.1± 0.4	3155 – 2373	1367.19±0.16	3.3± 0.4	2099 – 732
786.7 ±0.6	3.9± 3.3	1793 – 1006	1386.19±0.11	10.3± 0.8	2328 – 942
788.04±0.08	60.2± 4.6	1006 – 218	1404.16±0.25	2.2± 0.4	1693 – 289
801.62±0.09	10.0± 0.7	1020 – 218	1416.94±0.20	2.8± 0.4	2423 – 1006
818.29±0.15	5.0± 0.6	3146 – 2328	1428.70±0.21	3.2± 0.5	2936 – 1508
820.5 ±0.4	1.6± 0.5	2328 – 1508	1434.13±0.24	3.0± 0.5	1652 – 218
832.41±0.24	1.9± 0.4	2432 – 1599	1437.7 ±0.7	1.3± 0.5	1831 – 393
847.45±0.12	4.5± 0.4	2585 – 1738	1448.7 ±0.3	1.9± 0.4	1738 – 289
879.74±0.18	2.7± 0.4	1395 – 515	1453.32±0.10	8.6± 0.7	2185 – 732

TABLE I. (*Continued*).

Energy (keV)	Relative intensity[a]	Placement (keV)	Energy (keV)	Relative intensity[a]	Placement (keV)
1458.98 ± 0.22	2.8 ± 0.5	2967 – 1508	2192.32 ± 0.13	6.0 ± 0.5	2585 – 393
1490.0 ± 0.4	4.4 ± 1.2	2510 – 1020	2204.6 ± 0.6	0.8 ± 0.4	2423 – 218
1503.1 ± 0.6	2.5 ± 1.2	3155 – 1652	2227.28 ± 0.25	6.6 ± 1.5	2620 – 393
1520.17 ± 0.08	14.7 ± 0.9	1738 – 218	2238.4 ± 0.6	2.6 ± 0.4	2754 – 515
1540.8 ± 0.5	1.2 ± 0.4	2432 – 891	2249.7 ± 0.4	1.2 ± 0.3	
1543.6 ± 0.6	1.1 ± 0.3	3375 – 1831	2255.3 ± 0.7	1.6 ± 0.3	3146 – 891
1579.5 ± 0.4	3.6 ± 1.6	2585 – 1006	2291.61 ± 0.21	7.2 ± 0.5	2510 – 218
1584.7 ± 0.4	2.8 ± 0.4	2099 – 515	2304.97 ± 0.16	5.2 ± 0.5	2304 – 0
1609.3 ± 0.4	1.8 ± 0.4	3208 – 1599	2328.80 ± 0.09	11.3 ± 0.7	2328 – 0
1612.4 ± 0.4	2.6 ± 0.5	1831 – 218	2366.97 ± 0.22	2.4 ± 0.3	2585 – 218
1615.0 ± 0.3	2.8 ± 0.5	2754 – 1138	2403.75 ± 0.13	4.7 ± 0.4	2797 – 393
1641.7 ± 0.3	2.7 ± 0.5	3745 – 2103	2423.6 ± 0.4	0.8 ± 0.2	2423 – 0
1652.8 ± 0.3	2.0 ± 0.5	1652 – 0	2430.3 ± 0.6	0.7 ± 0.2	3372 – 942
1666.2 ± 0.6	0.8 ± 0.4	2852 – 1186	2437.8 ± 0.3	1.7 ± 0.3	2727 – 289
1670.33 ± 0.08	20.0 ± 1.1	2185 – 515	2451.6 ± 0.6	0.8 ± 0.3	2967 – 515
1681.1 ± 0.3	1.9 ± 0.4	3375 – 1693	2464.6 ± 0.5	2.0 ± 0.3	2754 – 289
1699.8 ± 0.3	1.9 ± 0.4	2432 – 732	2507.6 ± 0.6	1.4 ± 0.4	2797 – 289
1711.44 ± 0.17	4.1 ± 0.4	3504 – 1793	2510.41 ± 0.18	4.9 ± 0.5	2510 – 0
1722.6 ± 0.6	0.9 ± 0.4	3375 – 1652	2535.0 ± 0.5	1.1 ± 0.3	2754 – 218
1765.2 ± 0.6	0.8 ± 0.3	2980 – 1214	2574.04 ± 0.12	6.1 ± 0.5	2967 – 393
1773.84 ± 0.13	5.9 ± 0.5	2063 – 289	2578.9 ± 0.5	1.1 ± 0.3	2797 – 218
1776.9 ± 0.4	3.6 ± 0.4	2423 – 646	2613.7 ± 0.7	0.6 ± 0.3	3504 – 891
1786.6 ± 0.4	1.1 ± 0.4	2432 – 646	2633.75 ± 0.22	1.9 ± 0.3	2852 – 218
1790.85 ± 0.18	6.8 ± 0.9	2797 – 1006	2640.1 ± 0.6	0.6 ± 0.3	3372 – 732
1793.0 ± 0.5	2.2 ± 0.8	1793 – 0	2673.4 ± 0.5	1.0 ± 0.3	
1803.99 ± 0.25	2.2 ± 0.4	4227 – 2423	2693.4 ± 0.5	1.4 ± 0.4	3208 – 515
1814.1 ± 0.4	2.2 ± 0.5	2103 – 289	2736.7 ± 0.3	2.1 ± 0.4	3130 – 393
1816.7 ± 0.4	2.2 ± 0.5	1816 – 0	2754.2 ± 0.4	1.2 ± 0.3	2754 – 0
1831.5 ± 0.4	1.4 ± 0.4	1831 – 0	2761.6 ± 0.4	1.2 ± 0.3	2980 – 218
1851.8 ± 0.5	2.0 ± 0.6	3504 – 1652	2769.32 ± 0.12	5.3 ± 0.4	3775 – 1006
1854.5 ± 0.5	2.3 ± 0.6	2797 – 942	2790.89 ± 0.14	4.8 ± 0.4	
1857.6 ± 0.4	2.0 ± 0.5	2373 – 515	2815.03 ± 0.15	4.0 ± 0.4	3208 – 393
1862.4 ± 0.7	2.8 ± 2.0	2754 – 891	2832.8 ± 0.4	1.1 ± 0.2	4227 – 1395
1864.0 ± 0.4	4.5 ± 2.0	2510 – 646	2854.2 ± 0.4	1.6 ± 0.3	3745 – 891
1895.98 ± 0.09	11.0 ± 0.7	2185 – 289	2872.65 ± 0.25	2.2 ± 0.3	3815 – 942
1911.42 ± 0.21	2.2 ± 0.3	3372 – 1461	2886.6 ± 0.4	1.5 ± 0.3	
1935.1 ± 0.5	1.0 ± 0.3	2328 – 393	2903.8 ± 0.4	1.4 ± 0.3	3924 – 1020
1939.5 ± 0.3	1.5 ± 0.3	2585 – 646	2911.7 ± 0.4	1.2 ± 0.3	3130 – 218
1967.3 ± 0.3	2.3 ± 0.4	2185 – 218	2918.3 ± 0.3	2.2 ± 0.4	3924 – 1006
1979.57 ± 0.11	9.5 ± 0.8	2373 – 393	2936.2 ± 0.5	1.0 ± 0.3	2936 – 0
1994.2 ± 0.4	1.9 ± 0.5	2936 – 942	2941.8 ± 0.3	1.4 ± 0.3	
2006.8 ± 0.4	1.8 ± 0.4	3745 – 1738	2989.4 ± 0.4	1.3 ± 0.3	3504 – 515
2015.11 ± 0.17	2.8 ± 0.3	2304 – 289	3028.6 ± 0.4	1.2 ± 0.3	
2021.8 ± 0.4	1.3 ± 0.3	2754 – 732	3110.8 ± 0.7	0.7 ± 0.4	3504 – 393
2025.1 ± 0.5	1.3 ± 0.3	2967 – 942	3130.6 ± 0.6	1.4 ± 0.5	3130 – 0
2039.1 ± 0.4	1.3 ± 0.4	2328 – 289	3146.6 ± 0.3	1.1 ± 0.2	3146 – 0
2063.90 ± 0.12	7.5 ± 0.6	2063 – 0	3156.3 ± 0.4	0.8 ± 0.2	3155 – 0
2085.91 ± 0.10	12.0 ± 0.8	2304 – 218	3168.7 ± 0.4	1.1 ± 0.2	3815 – 646
2099.48 ± 0.20	2.3 ± 0.3	2099 – 0	3214.8 ± 0.5	0.7 ± 0.2	3504 – 289
2103.7 ± 0.6	1.0 ± 0.3	2103 – 0	3375.51 ± 0.19	2.7 ± 0.3	3375 – 0
2110.12 ± 0.13	5.2 ± 0.4	2328 – 218	3424.8 ± 0.5	1.3 ± 0.4	
2116.88 ± 0.11	5.8 ± 0.4	2510 – 393	3504.7 ± 0.3	1.2 ± 0.2	3504 – 0

[a] Measured relative to the 218.59 keV transition. The relative intensity can be converted to transitions per 100 β decays using the factor 0.0520, as calculated from the ^{139}Xe decay scheme with a ground-state β branching of 21%.

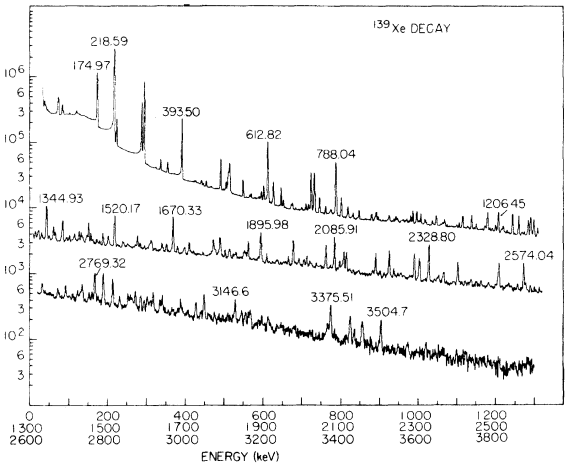

FIG. 1. γ-ray spectrum from the decay of ^{139}Xe.

presented here are mainly consistent with these tabulations and reflect subsequent reevaluation of the gated spectra which resulted in some minor changes to the preliminary level schemes.[22,29]

III. DATA AND RESULTS

The results of the studies on the decays of ^{139}Xe and ^{139}Cs are summarized in the tables and figures which follow. For each decay a table is presented which lists the observed γ-ray energies and relative intensities along with the errors in these quantities. Also included is the placement of the transition in the level scheme proposed in this work. A second table presented for each decay lists the level energies and their uncertainties, together with the deduced β branch to each level and the associated logft value with uncertainty.

A. ^{139}Xe Decay

Table I lists the energies and intensities for the γ-ray transitions observed following the ^{139}Xe decay. A representative spectrum is shown in Fig. 1.

The Q value for the β decay of ^{139}Xe was measured to be 5.02 ± 0.06 MeV.[1,30] This value is the weighted average of five different Q-value determinations based on end-point energy measurements of the β spectra in coincidence with the γ-ray transitions at 225.4, 296.5, 393.5, 612.8, and 788.0 keV.

The ground-state β branch in the decay of ^{139}Xe was deduced to be (21 ± 9)%. This value is based upon the intensities of the 218.6-keV transition following the decay of ^{139}Xe and the 1283.3-keV transition following the decay of ^{139}Cs, observed in the equilibrium decay spectrum

TABLE II. β branching and logft values for ^{139}Xe decay.

Level energy (keV)	β branching (%)	Logft [a]
0.0	21 ±9	6.67 ± 0.19 [b]
218.60 ± 0.08	~0	
289.79 ± 0.13	2.4 ±1.4	7.5 ±0.3 [b]
393.54 ± 0.07	16.3 ±2.0	6.63 ± 0.06
515.15 ± 0.18	20.7 ±2.1	6.47 ± 0.05
646.49 ± 0.08	0.19 ± 0.13	8.5 ±0.3 [b]
732.42 ± 0.06	2.16 ± 0.23	7.36 ± 0.05 [b]
891.6 ±0.3	~0	
942.50 ± 0.15	0.80 ± 0.15	7.70 ± 0.08 [b]
1006.50 ± 0.15	7.9 ±0.8	6.68 ± 0.05
1020.30 ± 0.13	1.33 ± 0.16	7.44 ± 0.05 [b]
1138.74 ± 0.09	0.20 ± 0.05	8.21 ± 0.11 [b]
1186.01 ± 0.20	0.15 ± 0.06	8.31 ± 0.17 [b]
1214.80 ± 0.12	0.41 ± 0.05	7.86 ± 0.06 [b]
1395.09 ± 0.21	0.30 ± 0.06	7.91 ± 0.09 [b]
1461.16 ± 0.22	0.53 ± 0.07	7.63 ± 0.06 [b]
1508.08 ± 0.12	0.14 ± 0.09	8.2 ±0.3 [b]
1599.90 ± 0.18	~0	
1652.78 ± 0.10	1.33 ± 0.16	7.12 ± 0.06 [b]
1693.91 ± 0.25	0.54 ± 0.10	7.49 ± 0.08 [b]
1738.58 ± 0.15	1.48 ± 0.15	7.03 ± 0.05 [b]
1793.04 ± 0.18	~0	
1816.4 ±0.3	0.15 ± 0.07	7.98 ± 0.20 [b]
1831.35 ± 0.23	0.09 ± 0.07	8.2 ±0.3 [b]
2063.81 ± 0.12	~0	
2099.58 ± 0.11	0.37 ± 0.06	7.42 ± 0.07 [b]
2103.58 ± 0.14	0.12 ± 0.07	7.91 ± 0.25 [b]
2119.49 ± 0.18	1.3 ±0.3	6.86 ± 0.10
2185.64 ± 0.17	2.53 ± 0.23	6.53 ± 0.04
2304.69 ± 0.25	1.52 ± 0.15	6.68 ± 0.05
2328.73 ± 0.11	1.29 ± 0.14	6.73 ± 0.05
2373.06 ± 0.15	0.69 ± 0.09	6.97 ± 0.06
2423.58 ± 0.24	0.21 ± 0.06	7.46 ± 0.13 [b]
2432.4 ±0.3	0.32 ± 0.05	7.27 ± 0.07 [b]
2510.38 ± 0.09	1.39 ± 0.17	6.57 ± 0.06
2585.88 ± 0.15	1.29 ± 0.15	6.55 ± 0.06
2620.8 ±0.4	0.48 ± 0.11	6.96 ± 0.10
2727.54 ± 0.17	0.20 ± 0.06	7.26 ± 0.13 [b]
2754.0 ±0.3	0.78 ± 0.14	6.64 ± 0.08
2797.30 ± 0.12	0.84 ± 0.10	6.58 ± 0.06
2852.28 ± 0.16	0.26 ± 0.04	7.04 ± 0.07
2936.63 ± 0.22	0.16 ± 0.07	7.18 ± 0.19
2967.43 ± 0.24	0.56 ± 0.07	6.61 ± 0.06
2980.32 ± 0.25	0.22 ± 0.04	7.01 ± 0.08
3130.31 ± 0.23	0.24 ± 0.04	6.84 ± 0.08
3146.90 ± 0.18	0.40 ± 0.06	6.60 ± 0.07
3155.93 ± 0.21	0.57 ± 0.09	6.44 ± 0.07
3208.64 ± 0.20	0.37 ± 0.05	6.58 ± 0.07
3372.62 ± 0.22	0.24 ± 0.04	6.60 ± 0.08
3375.24 ± 0.23	0.59 ± 0.07	6.21 ± 0.06
3504.56 ± 0.15	0.52 ± 0.06	6.13 ± 0.06
3745.36 ± 0.19	0.44 ± 0.06	5.91 ± 0.07
3775.72 ± 0.23	0.36 ± 0.04	5.96 ± 0.06
3815.16 ± 0.24	0.17 ± 0.03	6.23 ± 0.09
3924.6 ±0.3	0.25 ± 0.04	5.91 ± 0.08
4227.78 ± 0.24	0.33 ± 0.06	5.28 ± 0.10

[a] Calculated from proposed decay scheme, using Q_β = 5.02 ± 0.06 MeV.

[b] Logf_1t > 8.5, so cannot exclude first-forbidden unique β transition.

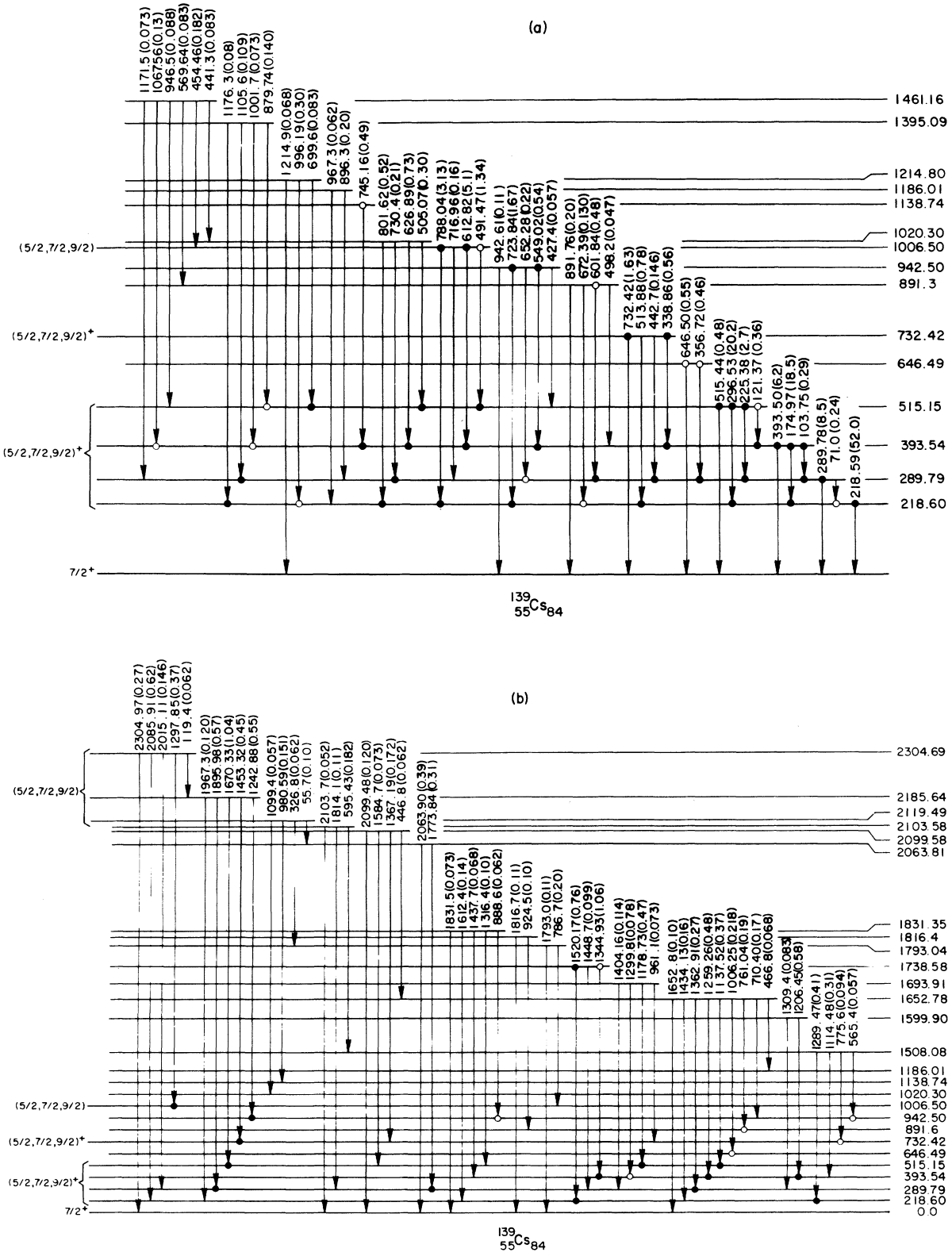

FIG. 2. Level scheme of ^{139}Cs populated in the decay of ^{139}Xe. (a) Levels to 1461 keV; (b) levels from 1508 to 2304 keV; (c) levels from 2328 to 2936 keV; (d) levels from 2967 to 4227 keV.

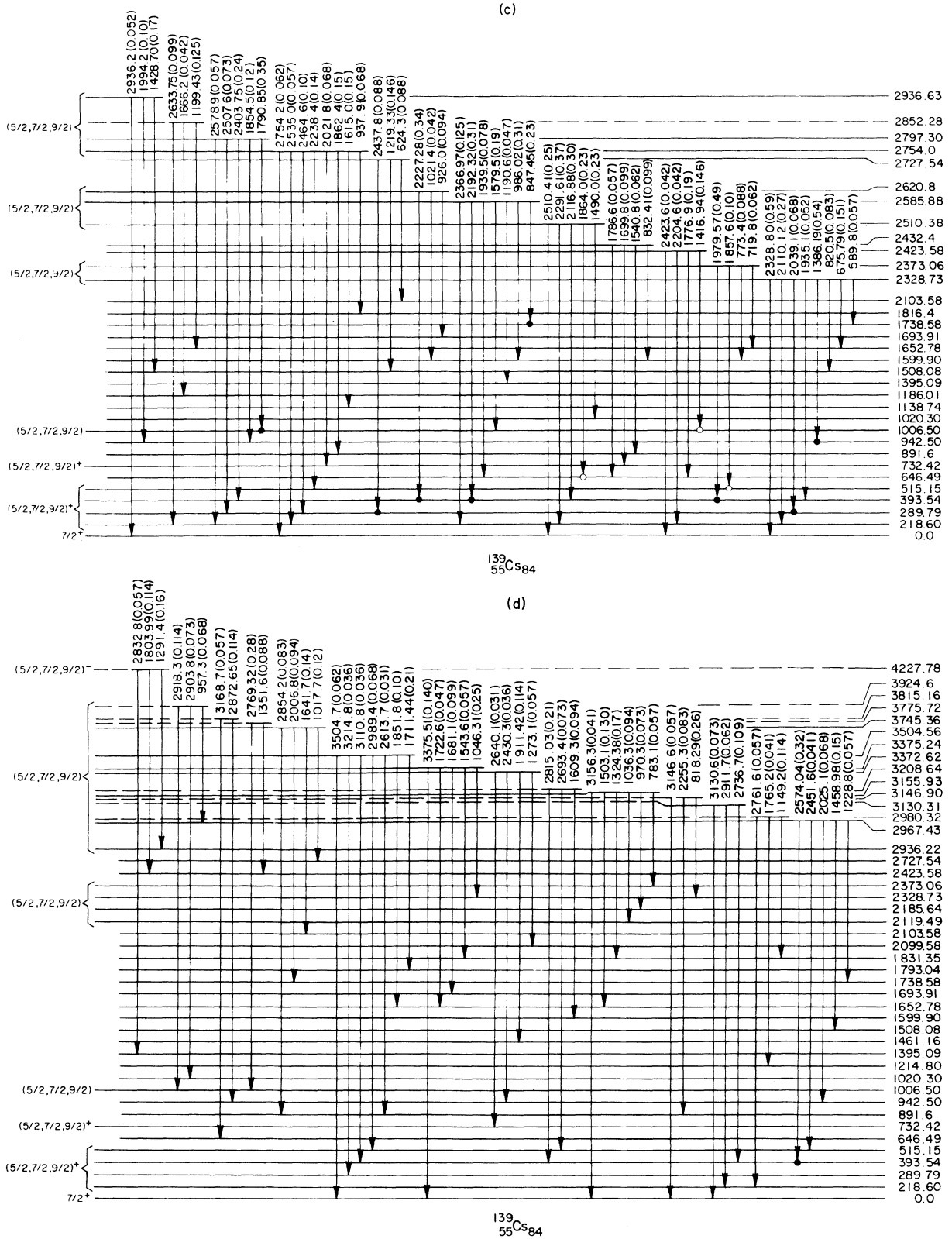

FIG. 2. *(Continued).*

TABLE III. Photopeaks observed in the decay of ^{139}Cs.

Energy (keV)	Relative intensity[a]	Placement (keV)	Energy (keV)	Relative intensity[a]	Placement (keV)
188.88 ± 0.20	1.1 ± 0.2	1887 – 1698	883.5 ± 0.3	1.8 ± 0.5	2166 – 1283
196.51 ± 0.18	1.2 ± 0.2	2877 – 1680	890.54 ± 0.08	10.2 ± 0.7	2173 – 1282
230.76 ± 0.09	4.3 ± 0.4	1538 – 1308	924.96 ± 0.08	9.2 ± 0.7	2605 – 1680
233.45 ± 0.22	1.3 ± 0.3	2110 – 1877	929.18 ± 0.06	32.0 ± 1.7	2349 – 1420
249.89 ± 0.18	1.4 ± 0.3	2349 – 2100	933.0 ± 0.3	1.8 ± 0.5	3464 – 2531
260.6 ± 0.4	1.0 ± 0.3	2680 – 1420	946.46 ± 0.08	13.7 ± 1.0	2229 – 1283
267.6 ± 0.3	1.3 ± 0.4	3701 – 3434	955.19 ± 0.19	4.0 ± 0.6	2375 – 1420
312.31 ± 0.21	1.1 ± 0.2	1620 – 1308	966.6 ± 0.3	2.4 ± 0.6	2249 – 1283
339.4 ± 0.4	0.8 ± 0.3	2156 – 1817	973.0 ± 0.4	1.8 ± 0.6	3434 – 2461
357.01 ± 0.16	1.9 ± 0.3	2037 – 1680	1040.93 ± 0.22	4.4 ± 0.4	2461 – 1420
375.91 ± 0.07	5.4 ± 0.4	2605 – 2229	1059.9 ± 0.3	2.1 ± 0.7	3665 – 2605
396.9 ± 0.3	2.2 ± 0.6	1817 – 1420	1063.7 ± 0.4	1.4 ± 0.7	2997 – 1933
401.08 ± 0.22	1.4 ± 0.3	2218 – 1817	1067.06 ± 0.19	3.3 ± 0.6	2605 – 1538
404.61 ± 0.25	1.1 ± 0.3		1076.94 ± 0.17	3.6 ± 0.7	2158 – 1081
416.49 ± 0.22	1.7 ± 0.4	2349 – 1933	1092.23 ± 0.12	5.8 ± 0.3	2375 – 1283
419.3 ± 0.3	1.3 ± 0.4	2100 – 1680	1108.93 ± 0.18	5.6 ± 0.8	2529 – 1420
430.20 ± 0.16	5.0 ± 0.4	2110 – 1680	1110.9 ± 0.4	2.7 ± 0.7	2531 – 1420
434.23 ± 0.20	1.9 ± 0.4	2524 – 2089	1120.89 ± 0.10	6.5 ± 0.6	1748 – 627
448.76 ± 0.12	4.2 ± 0.5	2605 – 2156	1159.30 ± 0.17	3.7 ± 0.5	3464 – 2304
454.66 ± 0.06	18.2 ± 1.1	1081 – 627	1178.35 ± 0.09	9.3 ± 0.8	2461 – 1283
466.70 ± 0.12	2.8 ± 0.3	1887 – 1420	1185.21 ± 0.17	4.1 ± 0.6	2605 – 1420
505.4 ± 0.3	1.3 ± 0.4	2605 – 2100	1190.42 ± 0.06	25.6 ± 1.5	1817 – 627
515.86 ± 0.07	7.2 ± 0.6	2605 – 2089	1216.14 ± 0.19	2.9 ± 0.5	2524 – 1308
528.20 ± 0.10	5.0 ± 1.7	2461 – 1933	1240.93 ± 0.25	2.1 ± 0.4	2524 – 1283
531.98 ± 0.04	29.7 ± 1.6	2349 – 1817	1249.41 ± 0.22	2.1 ± 0.4	3270 – 2020
538.35 ± 0.24	1.8 ± 0.4	2218 – 1680	1283.23 ± 0.05	1000 ± 53	1283 – 0
542.71 ± 0.15	3.2 ± 0.4	1850 – 1308	1306.09 ± 0.11	14.7 ± 1.3	1933 – 627
558.1 ± 0.3	1.2 ± 0.4	2375 – 1817	1308.13 ± 0.06	52 ± 3	1308 – 0
567.72 ± 0.05	13.7 ± 1.1	1850 – 1283	1316.4 ± 0.4	1.8 ± 0.5	2997 – 1680
567.72 ± 0.05	5.0 ± 1.1	2605 – 2037	1321.77 ± 0.06	32.5 ± 1.8	1949 – 627
594.02 ± 0.05	9.8 ± 0.6	1877 – 1283	1344.4 ± 0.4	1.7 ± 0.5	3434 – 2089
598.17 ± 0.18	1.6 ± 0.3	2218 – 1620	1353.92 ± 0.19	3.0 ± 0.5	3464 – 2110
601.48 ± 0.05	8.9 ± 0.5	2349 – 1748	1386.85 ± 0.24	2.6 ± 0.5	
604.22 ± 0.06	5.9 ± 0.4	1887 – 1283	1393.2 ± 0.3	2.1 ± 0.5	2020 – 627
613.4 ± 0.3	2.1 ± 0.6	2994 – 2380	1410.58 ± 0.07	20.9 ± 1.2	2037 – 627
616.91 ± 0.21	3.3 ± 0.6	2037 – 1420	1420.66 ± 0.06	110 ± 6	1420 – 0
619.7 ± 0.3	2.2 ± 0.6	2158 – 1538	1462.43 ± 0.19	5.0 ± 0.8	2089 – 627
627.24 ± 0.03	214 ± 11	627 – 0	1472.6 ± 0.5	1.6 ± 0.7	2100 – 627
651.08 ± 0.07	6.4 ± 0.5	2349 – 1698	1500.5 ± 0.3	2.0 ± 0.5	3674 – 2173
656.58 ± 0.13	4.3 ± 0.5	2605 – 1949	1529.3 ± 0.3	3.6 ± 0.8	2156 – 627
666.07 ± 0.11	4.0 ± 0.4	1749 – 1081	1531.2 ± 0.3	3.0 ± 0.8	2158 – 627
668.97 ± 0.08	5.8 ± 0.5	2349 – 1680	1539.09 ± 0.14	4.0 ± 0.4	1538 – 0
672.21 ± 0.15	2.7 ± 0.4	2605 – 1933	1546.63 ± 0.13	4.2 ± 0.5	2173 – 627
690.04 ± 0.09	3.0 ± 0.3	1998 – 1308	1563.9 ± 0.4	1.4 ± 0.4	3674 – 2110
714.90 ± 0.06	9.9 ± 0.6	1998 – 1283	1564.63 ± 0.13	4.2 ± 0.5	2847 – 1283
728.38 ± 0.09	5.6 ± 0.5	2605 – 1877	1573.84 ± 0.15	3.5 ± 0.4	2994 – 1420
735.68 ± 0.09	8.9 ± 0.7	1817 – 1081	1591.73 ± 0.11	7.3 ± 0.6	2218 – 627
737.60 ± 0.12	6.0 ± 0.6	2020 – 1283	1600.7 ± 0.5	2.7 ± 1.0	3950 – 2349
770.56 ± 0.19	2.3 ± 0.4	2079 – 1308	1620.74 ± 0.06	58 ± 3	1620 – 0
773.5 ± 0.3	1.3 ± 0.4		1677.44 ± 0.10	12.4 ± 0.9	2304 – 627
788.3 ± 0.4	1.2 ± 0.4	2605 – 1817	1680.72 ± 0.06	84 ± 4	1680 – 0
793.28 ± 0.07	10.5 ± 0.7	1420 – 627	1689.04 ± 0.25	2.7 ± 0.5	2997 – 1308
798.01 ± 0.14	3.6 ± 0.5	2218 – 1420	1698.66 ± 0.07	24.6 ± 1.4	1698 – 0
806.32 ± 0.21	1.7 ± 0.3	2089 – 1283	1711.09 ± 0.11	10.9 ± 0.8	2994 – 1283
827.52 ± 0.07	15.2 ± 1.0	2110 – 1283	1713.6 ± 0.4	2.2 ± 0.6	2997 – 1283
832.2 ± 0.3	1.7 ± 0.6	2649 – 1817	1722.55 ± 0.09	10.4 ± 0.7	2349 – 627
849.7 ± 0.3	1.4 ± 0.4	2847 – 1998	1737.9 ± 0.3	4.2 ± 0.4	3418 – 1680
858.4 ± 0.3	1.6 ± 0.4	2166 – 1308	1748.6 ± 0.3	2.1 ± 0.4	1748 – 0

TABLE III. (*Continued*).

Energy (keV)	Relative intensity [a]	Placement (keV)	Energy (keV)	Relative intensity [a]	Placement (keV)
1768.19 ± 0.21	1.9 ± 0.3	3701 – 1933	2380.66 ± 0.07	26.0 ± 1.5	2380 – 0
1793.63 ± 0.17	3.0 ± 0.4	3950 – 2156	2418.9 ± 0.4	1.7 ± 0.4	3701 – 1283
1814.6 ± 0.4	1.7 ± 0.5	3701 – 1887	2422.16 ± 0.18	4.0 ± 0.5	
1818.5 ± 0.3	2.1 ± 0.5	3839 – 2020	2524.47 ± 0.22	3.9 ± 0.6	2524 – 0
1850.7 ± 0.4	1.4 ± 0.4	1850 – 0	2529.9 ± 0.3	11 ± 3	2529 – 0
1877.45 ± 0.07	47.3 ± 2.5	1877 – 0	2531.84 ± 0.07	58 ± 4	2531 – 0
1887.57 ± 0.07	30.5 ± 1.7	1887 – 0	2605.75 ± 0.06	33.8 ± 1.9	2605 – 0
1904.50 ± 0.07	17.1 ± 1.0	2531 – 627	2649.32 ± 0.07	23.2 ± 1.3	2649 – 0
1933.48 ± 0.07	33.9 ± 1.8	1933 – 0	2673.98 ± 0.18	4.8 ± 0.6	
1949.26 ± 0.14	4.6 ± 0.5	1949 – 0	2774.04 ± 0.13	4.1 ± 0.4	3401 – 627
1998.46 ± 0.15	4.0 ± 0.4	1998 – 0	2836.88 ± 0.16	3.8 ± 0.4	3464 – 627
2003.4 ± 0.3	2.0 ± 0.4	3701 – 1698	2847.63 ± 0.08	13.8 ± 0.8	2847 – 0
2020.76 ± 0.25	18 ± 6	2020 – 0	2978.99 ± 0.24	1.8 ± 0.2	
2022.1 ± 0.5	9.0 ± 6.0	2649 – 627	2997.32 ± 0.09	11.9 ± 0.8	2997 – 0
2038.10 ± 0.11	5.9 ± 0.5	2037 – 0	3047.29 ± 0.16	4.1 ± 0.4	3674 – 627
2079.33 ± 0.19	5.8 ± 0.7	2079 – 0	3096.4 ± 0.4	1.2 ± 0.3	
2089.91 ± 0.09	18.9 ± 1.2	2089 – 0	3171.57 ± 0.23	2.5 ± 0.3	
2100.13 ± 0.17	6.5 ± 0.8	2100 – 0	3270.2 ± 0.3	1.4 ± 0.2	3270 – 0
2110.91 ± 0.06	91 ± 5	2110 – 0	3323.66 ± 0.15	6.9 ± 0.7	3950 – 627
2156.94 ± 0.13	5.7 ± 0.6	2156 – 0	3364.23 ± 0.11	11.0 ± 0.8	
2166.7 ± 0.4	1.7 ± 0.5	2166 – 0	3418.77 ± 0.15	5.5 ± 0.5	3418 – 0
2173.98 ± 0.07	27.8 ± 1.5	2173 – 0	3464.34 ± 0.09	15.1 ± 0.9	3464 – 0
2218.91 ± 0.23	2.9 ± 0.4	2218 – 0	3645.70 ± 0.13	3.8 ± 0.3	
2229.9 ± 0.3	1.9 ± 0.4	2229 – 0	3665.61 ± 0.08	18.9 ± 1.1	3665 – 0
2249.7 ± 0.4	1.6 ± 0.4	2249 – 0	3724.20 ± 0.15	3.6 ± 0.3	3724 – 0
2269.5 ± 0.3	2.0 ± 0.4		3769.16 ± 0.11	6.2 ± 0.4	3769 – 0
2304.97 ± 0.16	4.2 ± 0.5	2304 – 0	3819.99 ± 0.24	1.5 ± 0.2	3819 – 0
2330.2 ± 0.6	1.4 ± 0.6	3950 – 1620	3739.78 ± 0.17	2.5 ± 0.2	3839 – 0
2339.4 ± 0.5	3.9 ± 0.9		3853.87 ± 0.16	2.7 ± 0.2	3853 – 0
2349.92 ± 0.06	77 ± 4	2349 – 0	3887.8 ± 0.3	1.1 ± 0.2	3887 – 0
2352.6 ± 0.6	3.1 ± 1.1	3434 – 1081	3912.21 ± 0.21	1.7 ± 0.2	3912 – 0
2375.95 ± 0.11	9.6 ± 0.8	2375 – 0			

[a] Measured relative to the 1283.23 keV transition. The relative intensity can be converted to transitions per 100 β decays using the factor 0.007 72, as calculated from the ^{139}Cs decay scheme with 83% ground-state β branching.

of these two activities, and upon the value of the absolute intensity of the 1283.2-keV transition in the β decay of ^{139}Cs. The β branching intensities to the excited states of ^{139}Cs were calculated from the γ-ray intensity imbalances and the deduced ground-state β branch. These branching intensities were then used to calculate the logft values of the levels in ^{139}Cs; the results are shown in Table II.

The level scheme deduced for ^{139}Cs is shown in Fig. 2. The construction of the ^{139}Cs level scheme began with the partial level scheme proposed by Cook and Talbert, in which 48 transitions had been placed among 15 excited levels. Using the results of the γ-γ coincidence experiments and γ-ray energy sums, 13 of these levels were confirmed and a total of 213 of 220 observed transitions were placed among 55 excited levels, accounting for more than 99% of the observed γ-ray intensity. (Of the 34 excited levels below 2.5 MeV, 27 were established by coincidence information.) In the absence of coincidence information, energy agreement among at least 4 γ-ray cascades was required for the confident establishment of a level (other levels are illustrated as dashed lines which had good energy agreement for less than four placements).

B. ^{139}Cs Decay

The energies and intensities of the γ-ray transitions observed following the decay of ^{139}Cs are listed in Table III. A representative spectrum is seen in Fig. 3.

The β-γ coincidence experiments in the ^{139}Cs decay yielded a value of 4.29 ± 0.07 MeV for the Q value of this decay.[1] The γ-ray transitions at 454.7, 1190.4, 1283.2, 1321.8, 1620.7, 1680.7,

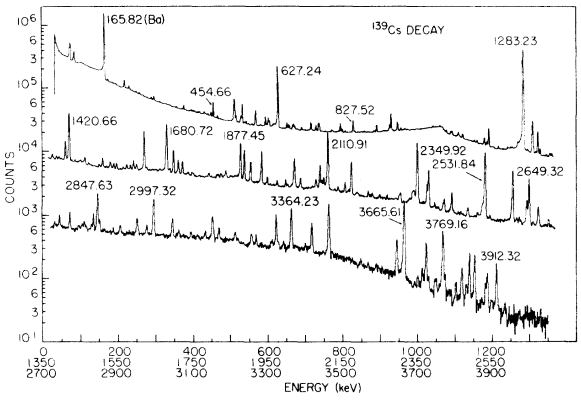

FIG. 3. γ-ray spectrum from the decay of ^{139}Cs.

1877.5, and 2110.9 keV were used in obtaining the gated β spectra. The resulting decay energies ranged from 4.20 to 4.36 MeV, with an rms spread of 0.06 MeV. Adding an uncertainty of 0.04 MeV in the calibration data leads to the error of 0.07 MeV quoted above. The value obtained here compares favorably to that reported by Monnand *et al.*[19] of 4.23 ± 0.10 MeV.

The ground-state β branch in the decay of ^{139}Cs was determined to be (83 ± 7)%. This value is based upon the relative intensities of the 1283.23-keV γ ray following the decay of ^{139}Cs and the 165.83-keV γ ray following the decay of ^{139}Ba. The integrated activity ratios of ^{139}Cs and ^{139}Ba were calculated from the moving tape collector parameters with the use of ISOBAR. The ground-state β branch for the decay of ^{139}Ba and the branch to the 165.83-keV state in ^{139}La have been determined earlier.[20] Monnand *et al.*[19] have calculated a value of (89.6 ± 1.0)% for the ^{139}Cs decay ground-state branch, basing their calculation on the intensities of the 1283.23-keV transition and the 165.83-keV transition observed following a chemical separation of the Ba formed during the collection of the ^{139}Xe source.

Our value for the ground-state β branch, the measured Q-value and γ-ray intensity balances

TABLE IV. β branching and logft values for ^{139}Cs decay.

Level energy (keV)	β branching (%)	Logft [a]	Level energy (keV)	β branching (%)	Logft [a]
0.0	83 ±7	6.94 ± 0.04 [b]	2249.79 ± 0.24	0.03 ± 0.01	9.04 ± 0.15 [b]
627.27 ± 0.07	~0	...	2304.83 ± 0.14	0.10 ± 0.04	8.47 ± 0.18 [b]
1081.96 ± 0.08	~0	...	2349.83 ± 0.09	1.3 ± 0.5	7.32 ± 0.17 [b]
1283.29 ± 0.09	6.8 ± 2.6	7.37 ± 0.17 [b]	2375.81 ± 0.19	0.16 ± 0.06	8.20 ± 0.17 [b]
1308.17 ± 0.07	0.24 ± 0.09	8.81 ± 0.16 [b]	2380.67 ± 0.07	0.18 ± 0.07	8.15 ± 0.17 [b]
1420.66 ± 0.12	0.40 ± 0.16	8.52 ± 0.18 [b]	2461.64 ± 0.08	0.13 ± 0.05	8.21 ± 0.17 [b]
1538.95 ± 0.13	0.03 ± 0.01	9.57 ± 0.15 [b]	2524.28 ± 0.13	0.08 ± 0.03	8.36 ± 0.17 [b]
1620.73 ± 0.06	0.43 ± 0.16	8.36 ± 0.16 [b]	2529.71 ± 0.17	0.13 ± 0.05	8.15 ± 0.17 [b]
1680.76 ± 0.09	0.43 ± 0.17	8.32 ± 0.17 [b]	2531.80 ± 0.09	0.59 ± 0.22	7.49 ± 0.17 [b]
1698.67 ± 0.06	0.12 ± 0.04	8.86 ± 0.15 [b]	2605.74 ± 0.06	0.66 ± 0.25	7.37 ± 0.17
1748.22 ± 0.15	0.03 ± 0.01	9.43 ± 0.15 [b]	2649.34 ± 0.10	0.26 ± 0.11	7.73 ± 0.19 [b]
1817.70 ± 0.13	~0		2847.70 ± 0.13	0.15 ± 0.06	7.75 ± 0.18 [b]
1850.96 ± 0.08	0.14 ± 0.05	8.69 ± 0.16 [b]	2994.38 ± 0.13	0.13 ± 0.05	7.64 ± 0.17 [b]
1877.39 ± 0.06	0.40 ± 0.15	8.21 ± 0.17 [b]	2997.28 ± 0.09	0.16 ± 0.06	7.54 ± 0.17
1887.53 ± 0.07	0.30 ± 0.11	8.33 ± 0.16 [b]	3270.23 ± 0.21	0.03 ± 0.01	7.89 ± 0.16
1933.46 ± 0.07	0.28 ± 0.11	8.32 ± 0.17 [b]	3401.31 ± 0.15	0.03 ± 0.01	7.67 ± 0.16
1949.12 ± 0.09	0.25 ± 0.10	8.36 ± 0.18 [b]	3418.75 ± 0.13	0.07 ± 0.01	7.27 ± 0.09
1998.24 ± 0.12	0.12 ± 0.05	8.64 ± 0.18 [b]	3434.42 ± 0.10	0.04 ± 0.02	7.48 ± 0.23
2020.80 ± 0.15	0.21 ± 0.09	8.38 ± 0.18 [b]	3464.36 ± 0.21	0.21 ± 0.08	6.71 ± 0.18
2037.92 ± 0.12	0.21 ± 0.08	8.37 ± 0.17 [b]	3665.61 ± 0.08	0.16 ± 0.06	6.40 ± 0.18
2079.0 ± 0.3	0.06 ± 0.02	8.88 ± 0.15 [b]	3674.58 ± 0.14	0.06 ± 0.02	6.81 ± 0.17
2089.87 ± 0.10	0.11 ± 0.04	8.61 ± 0.16 [b]	3701.93 ± 0.23	0.07 ± 0.03	6.67 ± 0.21
2100.08 ± 0.12	0.05 ± 0.02	8.94 ± 0.18 [b]	3724.20 ± 0.15	0.03 ± 0.01	6.98 ± 0.17
2110.87 ± 0.09	0.8 ± 0.3	7.73 ± 0.17 [b]	3769.16 ± 0.11	0.05 ± 0.02	6.64 ± 0.20
2156.96 ± 0.12	0.02 ± 0.01	9.29 ± 0.22 [b]	3819.99 ± 0.24	0.012 ± 0.005	7.11 ± 0.21
2158.77 ± 0.18	0.07 ± 0.03	8.75 ± 0.19 [b]	3839.78 ± 0.17	0.04 ± 0.01	6.52 ± 0.16
2166.70 ± 0.19	0.04 ± 0.02	8.98 ± 0.22 [b]	3853.87 ± 0.16	0.02 ± 0.01	6.78 ± 0.25
2173.94 ± 0.06	0.31 ± 0.12	8.09 ± 0.17 [b]	3887.75 ± 0.31	0.009 ± 0.004	7.01 ± 0.23
2218.91 ± 0.14	0.14 ± 0.05	8.40 ± 0.16 [b]	3912.32 ± 0.21	0.013 ± 0.005	6.76 ± 0.22
2229.80 ± 0.07	0.08 ± 0.03	8.63 ± 0.17 [b]	3950.79 ± 0.17	0.11 ± 0.04	5.68 ± 0.22

[a] Calculated from proposed decay scheme, using $Q_\beta = 4.29 \pm 0.07$ MeV.

[b] Log$f_1t > 8.5$, so cannot exclude first-forbidden unique β transition.

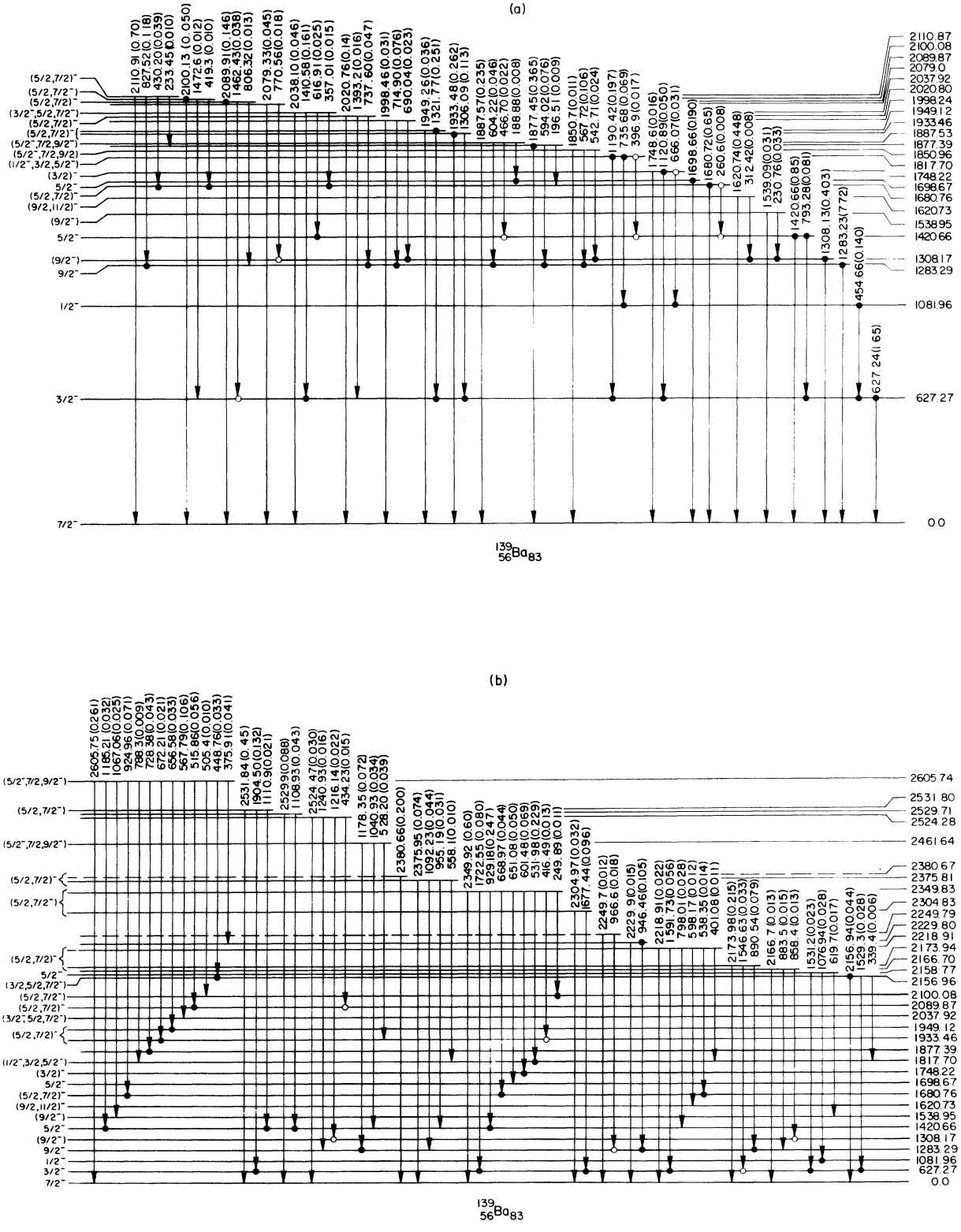

FIG. 4. Level scheme of ^{139}Ba populated in the decay of ^{139}Cs. (a) Levels to 2110 keV; (b) levels from 2156 to 2605 keV; (c) levels from 2649 to 3950 keV.

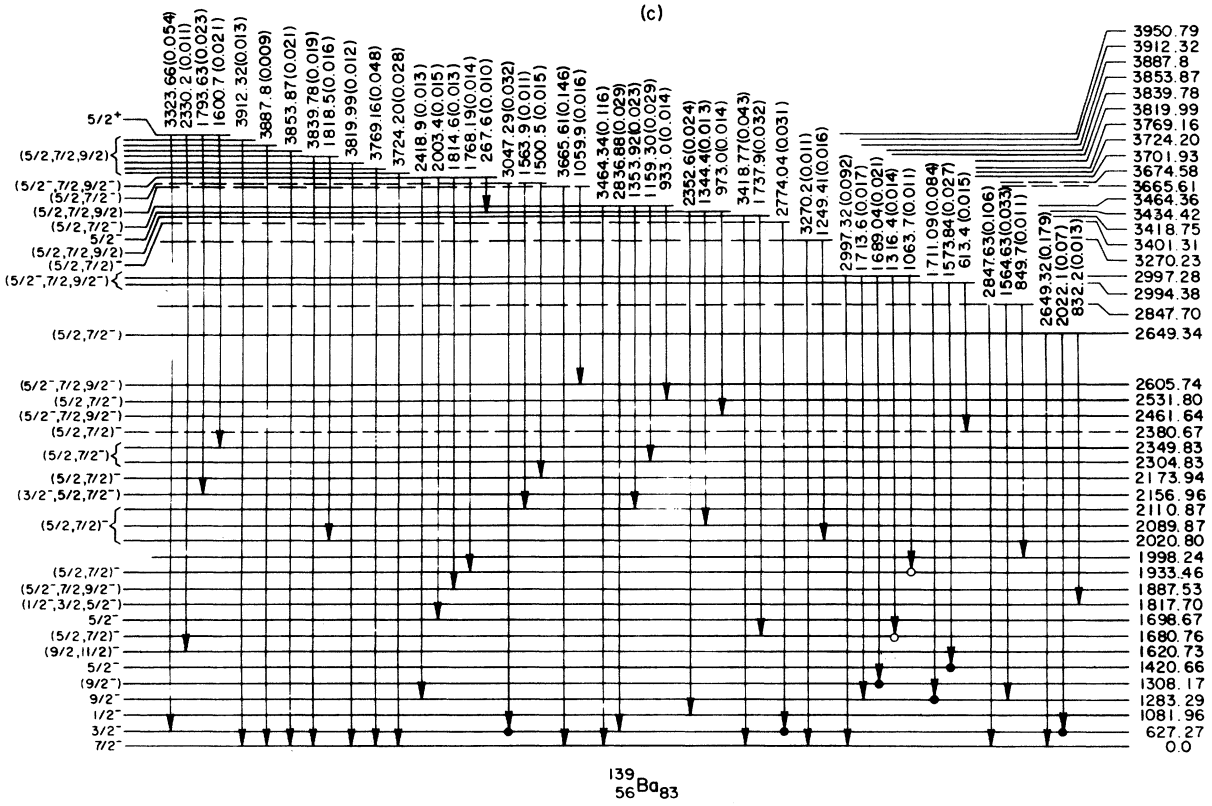

FIG. 4. (*Continued*).

resulting from the proposed decay scheme, was used to calculate log*ft* values for the β transitions presented in Table IV.

The level scheme deduced for ^{139}Ba is shown in Fig. 4. Several levels in ^{139}Ba have been established by the results of the (d,p) reaction experiments, and many of these levels were also populated in the β decay of ^{139}Cs. Through the use of the γ-γ coincidence information and energy sums a level scheme was constructed which contains 167 of the 179 observed transitions, placed among 59 excited levels and accounting for more than 99% of the γ-ray intensity. Of the 43 excited levels below 3 MeV, 40 were established through use of coincidence information. Several of the higher energy levels were established by the existence of γ-ray transitions which had to be placed as ground-state transitions due to decay energy considerations.

IV. DISCUSSION

A. ^{139}Cs Level scheme

Beyond the results obtained from studies of the ^{139}Xe decay, there is very little information concerning the levels of ^{139}Cs. No reaction work has been reported which would lead to levels in ^{139}Cs. As indicated previously,[6] the ground-state spin is $\frac{7}{2}$, and the parity is very likely positive as is the case for the nearby odd-A Cs isotopes,[31-36] shown in Fig. 5. This is consistent for the shell model since the protons above $Z=50$ have lowest-lying shell-model states $1g_{7/2}$ and $2d_{5/2}$.

The parent nucleus ^{139}Xe has 3 neutrons outside the major shell closure at $N=82$. The lowest-lying shell-model states available to these neutrons are $2f_{7/2}$ and $1h_{9/2}$, so the ^{139}Xe ground-state parity is very likely negative. Given the $\frac{7}{2}^+$ ground state of ^{139}Cs, the ground-state transition in the decay of ^{139}Xe, with $\log f_1 t \geq 8.5$, would indicate that the spin of the ^{139}Xe ground state, consistent with available shell-model states, is between $\frac{3}{2}$ and $\frac{9}{2}$. The systematics of the odd-A $N=85$ nuclei, shown in Fig. 6,[36-40] indicate that it is not unreasonable to assign a spin-parity for ^{139}Xe of $\frac{3}{2}^-$, as was done by Achterberg *et al.*[5] However, we have chosen a spin-parity of $\frac{7}{2}^-$ on the basis of the ground-state β branch log*ft* of 6.67, whereas Achterberg *et al.* used previous information[2] from which it was assumed that no ground-state β branch existed. This assignment, coupled with

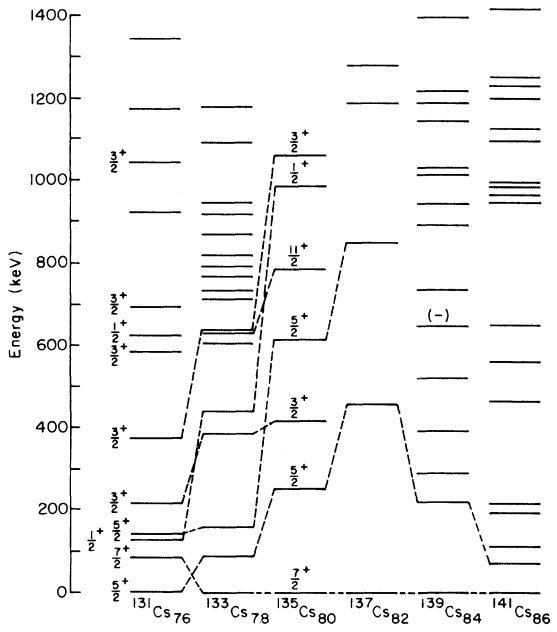

FIG. 5. Systematics of low-lying Cs levels, $A \geq 131$.

the appearance of the $N = 85$ systematics, indicates that the location of the $2f_{7/2}$ neutron state, relative to the Fermi level, is perturbed by the filling of the $1g_{7/2}$ proton state to only four protons.

Excited-state spin-parity range assignments in ^{139}Cs are made mainly from logft values, with the exception of a few states for which the depopulating transition multipolarities have been reported.[5] $M1/E2$ multipolarities have been deduced, on the basis of internal conversion coefficient measurements, for the γ rays at 103, 174, 218, 289, 296, 338, 393, and 732 keV. This establishes positive parity for the levels at 218, 289, 393, 515, and 732 keV. The $M2/E3$ character reported for the 356-keV transition makes negative parity likely for the 646-keV level. In addition to parity constraints imposed by the reported multipolarities, the $M1$ admixtures restrict the spin changes associated with the respective transitions. In this discussion, it has been assumed that the 218-keV level has a tentative spin parity of $\frac{5}{2}^+$, as indicated in the systematics of Fig. 5. Relative γ-ray transition rates to the $\frac{5}{2}^+$ 218-keV level were utilized in limiting the spin-parity upper range of several levels to $\frac{9}{2}^+$ (e.g., 1006 through 1395 keV).

Given that only two levels appear to have unique spin-parity assignments, the interpretation of the ^{139}Cs levels is very limited; the ground state appears to have the proton shell-model configuration $\pi(1g_{7/2})^5$, while that of the first excited state at 218.60 keV may be $\pi[(1g_{7/2})^4(2d_{5/2})^1]$. Additional studies, such as angular correlation and/or reaction measurements, would be required to determine the character of additional levels.

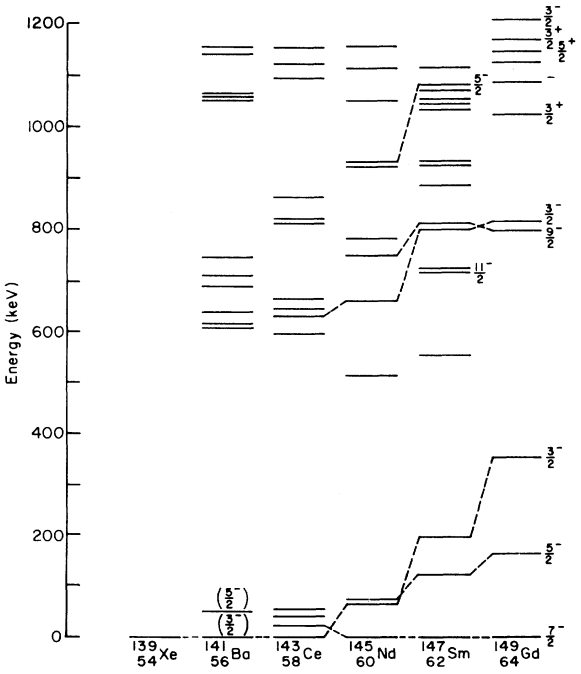

FIG. 6. Systematics of low-lying levels for $N = 85$ nuclei.

B. ^{139}Ba Level scheme

The parent nucleus ^{139}Cs has five protons outside the major shell $Z = 50$ and two neutrons outside the major shell $N = 82$. The measured value of $\frac{7}{2}$ for the ground-state spin leads to a shell-model configuration $\pi(1g_{7/2})^5\nu(2f_{7/2})^2$, with possible admixtures of other states. The β decay to the ground state of ^{139}Ba could then be considered as the decay of one of the $2f_{7/2}$ neutrons to a $1g_{7/2}$ proton. This first-forbidden transition is consistent with the 83% ground-state β branching observed in this decay leading to a logft value of 6.94. The ground state of ^{139}Ba appears to be a rather pure $2f_{7/2}$ neutron state, as indicated by the large spectroscopic factors found in (d,p) reaction experiments.[14] In addition, more than 99% of the β decay of ^{139}Ba proceeds to the $\frac{7}{2}^+$ ground state and $\frac{5}{2}^+$ first excited state in ^{139}La.[22]

There are excited states populated in ^{139}Ba in the decay of ^{139}Cs which have spins of $\frac{5}{2}^-$ and $\frac{9}{2}^-$ and which appear to be largely single particle in nature on the basis of reaction studies. These spins would indicate that the ground state of ^{139}Cs has some configuration mixing because the nature of the β-decay interaction would not allow these levels to be directly fed if the ground state were

a pure $\pi(1g_{7/2})^5\nu(2f_{7/2})^2$ configuration. Likely admixtures are $\pi(1g_{7/2})^5\nu(1h_{9/2})^2$, $\pi(1g_{7/2})^5\nu(2f_{5/2})^2$ and $\pi(1g_{7/2})^5\nu[(2f_{7/2})^1(1h_{9/2})^1]$. Carlson *et al.*[41] have discussed mixing in the ^{138}Xe ground state in terms of the configurations which could give rise to allowed β branches observed in the decay of ^{138}Xe. Their discussion is closely related to the decay of ^{139}Cs since the ^{138}Xe nucleus can be considered as the even-even core to which one proton is added to obtain ^{139}Cs. With the admixture of the configurations indicated above to the predominant $\pi(1g_{7/2})^5\nu(2f_{7/2})^2$ configuration in the ^{139}Cs ground state, it becomes plausible for the β decay to proceed to several of the states in ^{139}Ba within the framework of the β-decay interaction.

The 627-keV first excited state in ^{139}Ba has spin and parity of $\frac{3}{2}^-$. There is no measurable β branching to this level but the level is seen in the (d,p) reaction with $l_n=1$ transfer. The likely configuration is $\pi(1g_{7/2})^6\nu(3p_{3/2})^1$, consistent with both the reaction and decay data.

The second excited state occurs at an energy of 1081 keV and has spin and parity of $\frac{1}{2}^-$. As is the case with the first excited state there is no measurable β branching, but the level is populated in the (d,p) reaction with $l_n=1$. The likely configuration for this level is $\pi(1g_{7/2})^6\nu(3p_{1/2})^1$.

The level at 1283 keV is the most strongly fed of the excited states in ^{139}Ba in the β decay of ^{139}Cs, with a β branch of 6.8%. In the (d,p) experiments, this level is populated with $l_n=5$, and a spin and parity $\frac{9}{2}^-$ has been assigned on the basis of available shell-model states. The likely configuration is $\pi(1g_{7/2})^6\nu(1h_{9/2})^1$. The relatively large β feeding of this level suggests that the ground state of ^{139}Cs includes a substantial $\pi(1g_{7/2})^5\nu(1h_{9/2})^2$ component, from which the β decay proceeds as the decay of one of the $1h_{9/2}$ neutrons to a $1g_{7/2}$ proton. This β transition, which is first-forbidden, is consistent with the observed logft value of 7.4.

Another level which may be interpreted as primarily a single-particle excitation occurs at 1420 keV. This level is populated in (d,p) with $l_n=3$ and is assigned a spin and parity $\frac{5}{2}^-$. The probable configuration is $\pi(1g_{7/2})^6\nu(2f_{5/2})^2$. The β decay to this level could be described as the decay of a $2f_{5/2}$ neutron to a $1g_{7/2}$ proton, assuming the ^{139}Cs ground state includes a $\nu(2f_{5/2})^2$ component.

Although these lower-lying excited states appear to be primarily single-particle excitations they may also have admixtures of particle-core coupled states arising from a coupling of the 2^+ core vibration with the last neutron. Clement and Graw[42] have reported parentage coefficients for particle-core coupled states obtained through analysis of isobaric analog resonance experiments. In addition to the levels discussed above, they report parentage coefficients for the $\frac{9}{2}^-$ level at 1308 keV, the $\frac{7}{2}^-$ level at 1680 keV, the $\frac{5}{2}^-$ level at 1698 keV, and the $\frac{3}{2}^-$ level at 1748 keV, all of which are observed in this work. Additional levels in ^{139}Ba could arise from coupling of the two-phonon vibration or the octupole vibration in the core with the $2f_{7/2}$ neutron.

Carlson *et al.*[41] have studied the $N=82$ nucleus ^{138}Ba through the decay of ^{138}Cs. They have reported the energy of the 2^+ first-excited state as 1436 keV and the 4^+ second-excited state as 1899 keV. They report additional levels at energies of 2217, 2307, 2445, and 2369 keV which are fed by relatively strong β branches. The coupling of these excitations with the neutron single-particle excitations could lead to a large number of states with energies $\leq$2 MeV, and the complexity of this structure is such that one would need firm spin and parity assignments in order to sort out the various multiplets.

The spins and parities shown in the ^{139}Ba level scheme were derived from a variety of sources. For the levels which have large single-particle components the spins have been determined through reaction studies and shell-model considerations.[6,10-12,14,16] For levels observed in β decay but not identified with levels seen in reaction experiments, one can only determine a range of possible spins using the observed logft values and the rules of Raman and Gove.[21] In some cases, certain possible spins can be ruled out by the presence of transitions to levels of known spin and parity.

C. $N=83$ Systematics

Several experiments dealing with levels in $N=83$ nuclides have recently been performed.[42-46] In addition, recent unified model calculations have taken into account the $1i_{13/2}$ positive-parity single-particle state in these nuclides.[45,46] Earlier calculations included only the negative-parity single-particle states. Recent experiments using higher-energy deuterons[46] have shown that there are $\frac{13}{2}^+$ states in these nuclides at lower energies than was formerly thought to be the case. Other experiments have indicated that particle-core coupling plays an important part in levels below 2 MeV.[14,43,46]

Figure 7 shows the systematics of some of the excited states of the $N=83$ nuclides for which spins have been determined.[36,39,43,44,46] Reaction studies indicate that the ground states of all of these nuclides appear to be largely $2f_{7/2}$ single-

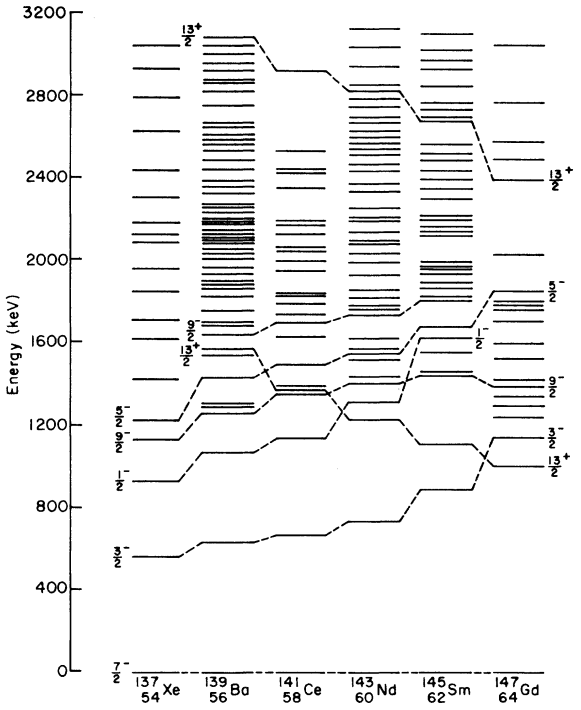

FIG. 7. Systematics of levels for N= 83 nuclei.

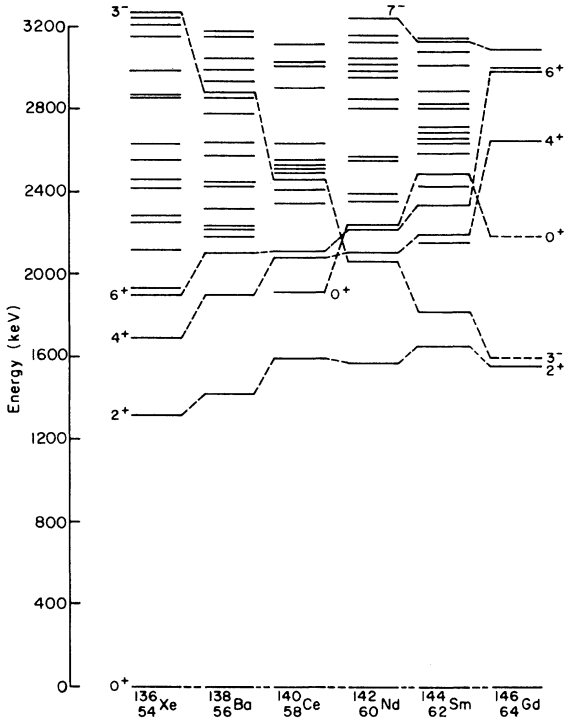

FIG. 8. Systematics of levels for N= 82 nuclei.

particle states, in agreement with the shell-model prediction of a single $2f_{7/2}$ neutron outside the $N = 82$ core.

Except for ^{147}Gd the first excited state in these nuclides is designated as the $3p_{3/2}$ single-particle state. This is based on the $l_n = 1$ neutron transfer observed in (d,p) experiments together with the conventional spin-orbit splitting of the shell model. The $3p_{1/2}$ state is the second excited state in the lighter of these nuclides but its energy increases rapidly with Z.

There are two sequences of $\frac{9}{2}^-$ levels in the figure. The lower of these, which includes the 1283-keV level in ^{139}Ba, is characterized primarily as the $1h_{9/2}$ single-particle excitation. The higher sequence of levels is due likely to a coupling of the $2f_{7/2}$ neutron with the 2^+ vibrational state in the $N = 82$ core nuclides, although one cannot rule out configuration mixing of the single-particle state and the particle-core coupled state in both of these levels.

A sequence of levels of spin and parity $\frac{13}{2}^+$ is shown in the figure, and for these levels the energy decreases with Z in contrast to the behavior of the single-particle states. It is interesting, in pursuit of this behavior, to compare the $N = 83$ systematics with the systematics of the $N = 82$ core nuclides[45,47-54] which are shown in Fig. 8. In the figure are shown the 2^+ and 4^+ vibrational states as well as the 3^- octupole state for these nuclides. The striking similarity between the behavior of the 3^- states and that of the $\frac{13}{2}^+$ states leads to speculation that the $\frac{13}{2}^+$ states arise from a stretched coupling of the 3^- core vibration with the $2f_{7/2}$ neutron. Additional components of these states could be the $1i_{13/2}$ single-particle excitation and a coupling of the $1h_{9/2}$ single particle with the 3^- core excitation. There is another sequence of $\frac{13}{2}^+$ levels in these nuclides which shows the same behavior with Z, but this sequence lies approximately 1500 keV higher in energy.[43] The $1i_{13/2}$ single-particle configuration may be a strong component of these states. It should be mentioned that the 1540-keV $\frac{13}{2}^+$ state in ^{139}Ba reported in (d,p) studies was not seen in this study and cannot be the 1538-keV level populated in β decay.

One striking feature of these nuclides is the high level density in the region between 1.0 and 2.5 MeV. Many of these states appear to arise from particle-core coupling between the $N = 82$ core and the single-neutron states and others could arise from the breaking of proton pairs in the core. Additional information, such as well-defined spins and parities of the levels, would be helpful in achieving a better understanding of the complex structure of these nuclides.

This work was supported by the U. S. Department of Energy under Contract No. W-7405-eng-82.

*Present address: EG&G Idaho, P.O. Box 1625, Idaho Falls, Idaho 83401.
†Present address: Los Alamos Scientific Laboratory, P.O. Box 1663, Los Alamos, N.M. 87545.

[1]J. P. Adams, G. H. Carlson, M. A. Lee, W. L. Talbert, Jr., F. K. Wohn, J. R. Clifford, and J. R. McConnell, Phys. Rev. C 8, 767 (1973).
[2]G. Holm, S. Borg, U. Fägerquist, and F. Kropff, Ark. Fys. 34, 447 (1967).
[3]T. Alväger, R. A. Naumann, R. F. Petry, G. Sidenius, and T. D. Thomas, Phys. Rev. 167, 1105 (1968).
[4]J. W. Cook and W. L. Talbert, Jr. (private communication).
[5]E. Achterberg, F. C. Iglesias, A. E. Jech, J. A. Moragues, D. Otero, M. L. Perez, A. N. Proto, J. J. Rossi, W. Scheuer, and J. F. Suarez, Phys. Rev. C 5, 1759 (1972).
[6]C. Ekström, S. Ingelman, G. Wannberg, and M. Skarestad, Hyperfine Interactions 4, 165 (1978).
[7]R. H. Fulmer, A. L. McCarthy, and B. L. Cohen, Phys. Rev. 128, 1302 (1962).
[8]F. W. Bingham and M. B. Sampson, Phys. Rev. 128, 1796 (1962).
[9]J. Rapaport and W. W. Buechner, Phys. Lett. 18, 299 (1965).
[10]C. A. Weidner, A. Heusler, J. Solf, and J. P. Wurm, Nucl. Phys. A103, 433 (1967).
[11]J. Rapaport and A. K. Kerman, Nucl. Phys. A119, 641 (1968).
[12]D. von Ehrenstein, G. C. Morrison, J. A. Nolen, Jr., and N. Williams, Phys. Rev. C 1, 2066 (1970).
[13]D. von Ehrenstein and M. C. Tsangarides, Bull. Am. Phys. Soc. 17, 511 (1972).
[14]S. S. Ipson, W. Booth, and J. G. B. Haigh, Nucl. Phys. A206, 114 (1973).
[15]J. A. Maragues, M. A. J. Mariscotti, W. Gelletly, and W. R. Kane, Phys. Rev. 180, 1105 (1969).
[16]P. von Brentano, N. Marquardt, J. P. Wurm, and S. A. A. Zaidi, Phys. Lett. 17, 124 (1965).
[17]V. A. Aksenov, E. B. Brodkin, A. V. Bushuev, and V. I. Polikarpov, At. Energ. 13, 271 (1972).
[18]E. A. Zherebin, A. I. Krylov, and V. I. Polikarpov, Yad. Fiz. 3, 981 (1966) [Sov. J. Nucl. Phys. 3, 717 (1966)].
[19]E. Monnand, J. Blachot, R. Brissot, L. C. Carraz, J. Crancon, C. Ristori, F. Schussler, and A. Moussa, CEA Report No. CEA-R-4499, Centre d'Etudes Nucleaires de Grenoble, 1973 (unpublished).
[20]G. Gleason (private communication to M. Martin).
[21]S. Raman and N. B. Gove, Phys. Rev. C 7, 1995 (1973).
[22]L. R. Greenwood, Nucl. Data Sheets 12, 139 (1974).
[23]J. R. McConnell and W. L. Talbert, Jr., Nucl. Instrum. Methods 128, 227 (1975).
[24]J. H. Norman, W. L. Talbert, Jr., and D. M. Roberts, USAEC Report No. IS-1893, Iowa State University, 1968 (unpublished).
[25]F. K. Wohn, J. R. Clifford, G. H. Carlson, and W. L. Talbert, Jr., Nucl. Instrum. Methods 101, 343 (1972).
[26]G. H. Carlson, W. C. Schick, Jr., W. L. Talbert, Jr., and F. K. Wohn, Nucl. Phys. A125, 267 (1969).
[27]W. C. Schick, Jr., USAEC Report No. IS-3460, Iowa State University, 1974 (unpublished).
[28]R. J. Olson, Ph.D. thesis, Iowa State University, 1971 (unpublished).
[29]M. A. Lee, Ph.D. thesis, Iowa State University, 1973 (unpublished).
[30]F. K. Wohn and W. L. Talbert, Jr., Phys. Rev. C 18, 2328 (1978).
[31]R. L. Auble, H. R. Hiddleston, and C. P. Browne, Nucl. Data Sheets 17, 573 (1976).
[32]E. A. Henry, Nucl. Data Sheets 11, 495 (1974).
[33]E. A. Henry, Nucl. Data Sheets 14, 191 (1975).
[34]R. L. Bunting, Nucl. Data Sheets 15, 335 (1975).
[35]W. R. Western, John C. Hill, W. L. Talbert, Jr., and W. C. Schick, Jr., Phys. Rev. C 15, 1024 (1977).
[36]J. K. Tuli, Nucl. Data Sheets 23, 529 (1978).
[37]J. F. Lemming, Nucl. Data Sheets 13, 229 (1974).
[38]T. W. Burrows, Nucl. Data Sheets 12, 203 (1974).
[39]B. Harmatz and W. B. Eubank, Nucl. Data Sheets 25, 113 (1978).
[40]S. V. Jackson, J. W. Starner, W. R. Daniels, M. E. Bunker, and R. A. Meyer, Phys. Rev. C 18, 1840 (1978).
[41]G. H. Carlson, W. L. Talbert, Jr., and J. R. McConnell, Phys. Rev. C 9, 283 (1974).
[42]H. Clement and G. Graw, Phys. Lett. 57B, 323 (1975).
[43]W. Booth and S. Wilson, Nucl. Phys. A247, 126 (1975).
[44]S. G. Prussin, R. G. Lanier, G. L. Struble, L. G. Mann, and S. M. Shoenung, Phys. Rev. C 16, 1001 (1977).
[45]Z. Haratym, J. Kownacki, J. Ludziejewski, Z. Sujkowski, L.-E. De Geer, A. Kerek, and H. Ryde, Nucl. Phys. A276, 299 (1976).
[46]W. Booth, S. Wilson, and S. S. Ipson, Nucl. Phys. A238, 301 (1975).
[47]R. L. Bunting and J. L. Kraushaar, Nucl. Data Sheets 13, 191 (1974).
[48]P. A. Moore, P. J. Riley, C. M. Jones, M. D. Mancusi, and J. L. Foster, Jr., Phys. Rev. 180, 1213 (1969).
[49]S. C. Pancholi and M. J. Martin, Nucl. Data Sheets 18, 167 (1976).
[50]L. K. Peker, V. M. Sigalov, and Yu. I. Kharitonov, Nucl. Data Sheets 12, 343 (1974).
[51]J. K. Tuli, Nucl. Data Sheets 25, 53 (1978).
[52]T. W. Burrows and R. L. Auble, Nucl. Data Sheets 16, 231 (1975).
[53]T. W. Burrows, Nucl. Data Sheets 14, 413 (1975).
[54]W. R. Western, John C. Hill, W. L. Talbert, Jr., and W. C. Schick, Jr., Phys. Rev. C 15, 1822 (1977).